Temperature dependence of the two-roton Raman spectrum of superfluid ^{4}He

Kohji Ohbayashi,* Masayuki Udagawa, and Norio Ogita
Faculty of Integrated Arts and Sciences, Hiroshima University, Higasihiroshima 739-8521, Japan
(Received 3 March 1998)

Temperature dependence of the two-roton Raman spectrum of superfluid ^{4}He was measured at pressures of saturated vapor pressure, 9.8×10^4 Pa, 4.9×10^5 Pa, and 1.96×10^6 Pa from the lowest temperature of 0.75 K to temperatures above the λ point. The temperature dependence of both the spectral shape and intensity of the two-roton peak has been found to be simulated well by a model, where the temperature effect is simply broadening of the spectrum with small variation of the roton minimum energy. Spectral shape and peak height at elevated temperatures have been found to be reproduced by convolution integrals of the spectrum at the lowest temperature with Lorentzian functions which take into account the temperature broadening effect at each temperature, where also small temperature dependence of the roton minimum energy had to be taken into account in order to fit the spectrum position. The fact verifies that the Raman spectral shape of superfluid ^{4}He does not change qualitatively at elevated temperatures and also even crossing the λ point. By the model analysis, temperature dependence of the roton minimum energy and the roton half width (inverse of the roton lifetime) have been determined at each pressure as a function of temperature. The results have been compared with theories. [S0163-1829(98)09029-8]

I. INTRODUCTION

The dynamical structure factor $S(q,\omega,T)$ is one of the central interests of superfluid ^{4}He. Most of the static and dynamical properties of superfluid ^{4}He can be explained by theoretical calculations based on the dispersion relation of elementary excitations and their interactions.[1–3] At the absolute zero of temperature, the structure factor has no width and is approximately written as[4]

$$S(q,\omega,0)=Z_s\delta(\omega-\varepsilon(q))+S_m(q,\omega,0). \tag{1}$$

The first term on the right-hand side is the single excitation contribution and the second is the multiphonon term. If we scan $Z_s\delta(\omega-\varepsilon(q))$ as a function of energy $\hbar\omega$ at a fixed momentum $\hbar q$, it is peaked at $\varepsilon(q)$ with zero width. $\varepsilon(q)$ as the function of q is the dispersion relation of elementary excitations. The second term, the multiphonon contribution, is broad even at absolute zero. In order to understand the properties of superfluid ^{4}He at an arbitrary temperature T based on the elementary excitations, the dispersion relation at finite T must be known. However, to deduce the dispersion relation at an arbitrary temperature from the observed $S(q,\omega,T)$ is not a straightforward task. The single excitation spectrum becomes markedly broad with an increase of temperature and it overlaps with the second multiphonon signal. Besides the experimental separation problem, a conceptional issue exists.

Concerning the temperature dependence of the $S(q,\omega,T)$, considerable attentions have been paid by theorists and neutron experimentalists. One of the questions is, because the λ transition of superfluid ^{4}He is associated with Bose-Einstein condensation, whether the dynamical structure factor changes qualitatively crossing the λ point or not.[5] Another problem is that, because the dynamical structure factor has the two-branch structure, how to separate the single-excitation peak from the multiphonon branch at elevated temperatures. In addition to the branch separation problem, another question is whether the normal fluid part remains in $S(q,\omega,T)$ observed for superfluid phase or not. And if it remains, the problem is how to estimate it and how to subtract it. Woods and Svensson proposed a two-component model that the one-phonon peak has a weight proportional to macroscopic superfluid density $\varrho_s(T)$.[6] On the other hand, Talbot *et al.* claimed the simple multiphonon subtraction model.[7] The work by Stirling and Glyde[8] reported different behavior at different wave vectors. A theoretical interpretation of their experimental results has been given by Glyde and Griffin.[9] Theoretically, Griffin proposed that Bose-Einstein condensation does not cause a drastic change to $S(q,\omega,T)$ and only abrupt narrowing is expected as we pass through the λ temperature from above.[10,11] The parameters of the elementary excitations, especially those of rotons, differ depending on what model we use for analysis. And, in spite of those extensive experimental and theoretical studies, interpretation of the temperature dependence of $S(q,\omega,T)$ observed by neutron scattering is not conclusive.[5] For an extensive review both on neutron and Raman scattering, we refer the readers to Griffin's recent book.[12]

Raman scattering from superfluid ^{4}He gives us information complementary to neutron scattering. In a simplified model, the Raman spectrum of liquid ^{4}He at temperature T as a function of the energy shift $\hbar\omega$ from the exciting laser is[4]

$$R(\omega,T)\propto\int\int t(\boldsymbol{q})t(\boldsymbol{q}')H(q,q',\omega,T)d\boldsymbol{q}d\boldsymbol{q}', \tag{2}$$

where $t(\boldsymbol{q})$ is called the light-helium coupling factor, which is a factor to express how much an excitation with wave vector $\boldsymbol{q}$ contributes to Raman scattering. $H(q,q',\omega,T)$ expresses how the Raman spectrum is related to the dynamical structure factor $S(q,\omega,T)$. In a simplified theoretical model, it is the convolution integral

$$H(q,q',\omega,T)=\int_{-\infty}^{\infty} S(q,\omega',T)S(q',\omega-\omega',T)d\omega'. \tag{3}$$

As mentioned above, temperature dependence of the dynamical structure factor $S(q,\omega,T)$ is directly observed by neutron inelastic scattering. This equation shows that it can also be studied by Raman scattering indirectly. Due to the convolution integral of Eq. (3), Raman peaks appear at energy shifts where the density of state is large. The density of state diverges at the two-roton and two-maxon energies. Then two peaks would be expected at these energy shifts. However, because the light-helium coupling factor $t(\boldsymbol{q})$ is very small at the two-maxon region, the only dominant peak in the Raman spectrum is the two-roton peak.[4,13] This simplifies interpretation of the Raman spectrum. The purpose of this work is to measure the temperature dependence of Raman spectrum at a few selected pressures, to clarify in which model it is explained, and to derive the temperature dependence of roton parameters.

In this paper measurements of the temperature dependence of the Raman spectrum of liquid ^{4}He at pressures of saturated vapor pressure (SVP), 9.8×10^4 Pa, 4.9×10^5 Pa, and 1.96×10^6 Pa are reported. The results are analyzed by a simple Lorentzian broadening model for temperature dependence of the dynamical structure factor. From the model analysis of the experimental data, temperature dependences of the energy and lifetime of rotons are determined. Those results are compared with theories.

II. EXPERIMENTAL APPARATUS

The schematic figure of the experimental optical system used in this experiment was shown in our preliminary report.[14] The incident light source was an argon-ion laser (Nippon Electric Company model No. GLG3200) operated at 514.5 nm with output power of 400 mW. Polarization of the beam from the source was vertical. To determine the direction of polarization of the beam incident on the sample arbitrarily, the polarization rotator and the polarizer were used. To reduce the tail of the central component at the two-roton Raman spectrum region, the direction of the incident beam polarization was set horizontal during measurement. The beam was focused into the cell with the lens, the focal length of which was 100 mm. The light scattered at right angles was gathered with the lens of f/3.7. The Dove prism adjusted the direction of the laser beam image to be parallel to the direction of the inlet slit of the spectrometer.

The double grating spectrometer was a JASCO CT1000D type. The imaging photon detector (a Surface Sciences Instruments model 2601A type) was used for simultaneous detection of the whole spectrum imaged on the two-dimensional surface of outlet slit position of the spectrometer. In order to calibrate weak nonlinearity in the energy shift versus position relation at the outlet slit position, the rotational Raman spectral peaks of N_2 and O_2 molecules in air were observed.[15] The accuracy of the energy shifts was ±0.06 cm^{-1}. The observed signals were transferred to the computer for analysis.

The Cu-Be sample cell was cooled with a recirculation type ^{3}He cryostat. The cell mounted on the bottom of a pumped liquid ^{3}He bath. Temperature was controlled with a calibrated Ge resister within an accuracy of ±15 mK. Helium entered the cell through a small capillary tube after being filtered by traps at liquid N_2 temperature and at liquid ^{4}He temperature to eliminate dust or ice particles.

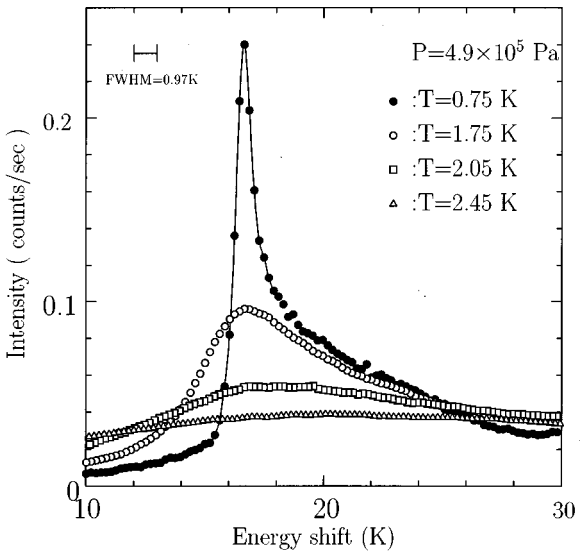

FIG. 1. Temperature dependence of the Raman spectrum of superfluid ^{4}He measured at the pressure of 4.9×10^5 Pa. The dominant peak is the two-roton Raman scattering. The instrumental full width at half maximum (FWHM) was 0.97 K. The width of the two-roton peak at $T=0.75$ K is determined by this instrumental width. As temperature increases, broadening of the spectrum, decrease of the peak height and the shift of the peak maximum to higher energy shift are observed.

III. RESULTS AND DISCUSSION

The results at 4.9×10^5 Pa are shown in Fig. 1 for temperatures of 0.75, 1.75, 2.05, and 2.45 K, with an instrumental full width at half maximum (FWHM) of 0.97 K. At SVP, measurement above the λ point was difficult due to local bubbling in the sample cell. The set of data at 4.9×10^5 Pa can show behavior both for superfluid and normal fluid. We made preliminary reports of the results at this pressure at LT19 conference and in a review article.[14,16] In this work, measurements are extended to other pressures. At 4.9×10^5 Pa also, remeasurements and reanalysis have been made. The temperature of 0.75 K was the lowest in this series of measurements. The dominant asymmetrical peak is the two-roton Raman scattering. The observed width of the peak was determined by the instrumental full width at half maximum (FWHM) at this temperature. The spectrum without instrumental broadening would appear much narrower in its width and stronger in peak height. At 1.75 K, the liquid is in the superfluid phase but the spectrum is broadened, still keeping the feature of the spectrum at the lowest temperature. At 2.05 K, the sample is in the superfluid phase near the λ transition and the spectrum is considerably broadened. At a temperature of 2.45 K above the λ transition, the spectrum is almost featureless. The maximum of the peak is shifted to about 20 K. The features of the temperature dependence are broadening, the decrease of the peak maximum and the shift of the

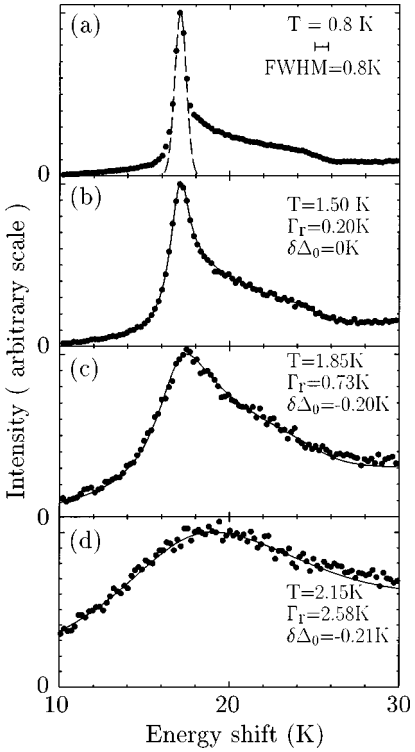

FIG. 2. Temperature dependence of the Raman spectrum of superfluid ^{4}He at SVP. The vertical scale is arbitrarily chosen so that the change of the spectral shape with temperature is clearly shown. The dominant peak is the two-roton Raman scattering. In (a) at $T=0.8$ K, the instrumental profile shown by the broken line determines the spectral width of the peak. The instrumental full width at half maximum was 0.8 K. The solid curves in the plots (b), (c), and (d) are the best fit convolution integral [Eq. (10) in the text] of the spectrum (a) with Lorentzian functions. Parameters Γ_r and $\delta\Delta_0$ determined by the best fit are written for each plot.

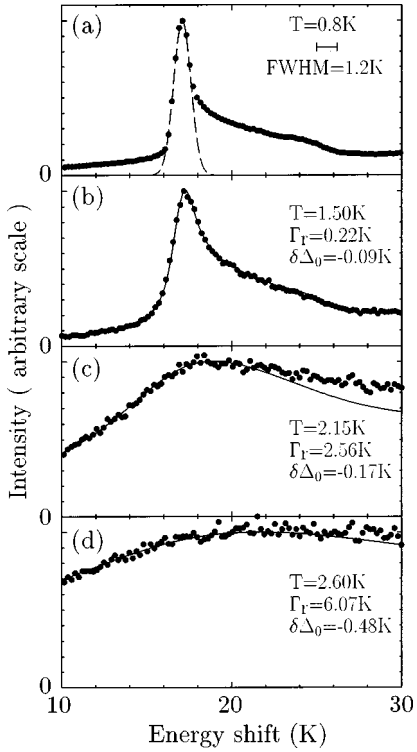

FIG. 3. Temperature dependence of the Raman spectrum of superfluid ^{4}He at the pressure of 9.8×10^4 Pa. The plot is similar to Fig. 2.

apparent peak maximum to higher energy as temperature increases.

The temperature dependences of the Raman spectrum are shown in Figs. 2, 3, 4, and 5 for respective pressures of SVP, 9.8×10^4 Pa, 4.9×10^5 and 1.96×10^6 Pa. In these figures, vertical scale is normalized for convenience to see the change of the spectral shape clearly. Temperature dependence of actual absolute intensity at different pressures are similar to that shown in Fig. 1. Temperature dependence at SVP was reported by Greytak and Yan.[18] The present data at SVP is consistent with theirs. We will discuss the temperature dependence of the two-roton peak, which is dominant in the spectrum.

The dispersion of rotons is[1,2]

$$\varepsilon_r(q)=\Delta_0+\frac{\hbar^2(q-q_0)^2}{2\mu_0}-\frac{\hbar^3|q-q_0|^3}{2\mu_0 k_i},\quad \begin{cases} k_i=1 & q<q_0 \\ k_i=2 & q\geqslant q_0, \end{cases} \tag{4}$$

where $\varepsilon_r(q)$ is the roton energy, Δ_0 is the roton minimum energy, q_0 is the roton momentum at the roton minimum, and μ_0 is the roton mass. The third term on the right is the cubic correction to the original Landau's form[1] by Bedell, Pines, and Fomin.[2] The dispersion is cutoff halfway between the maxon energy and the roton minimum.

The convolution integral of Eq. (3) enhances the part of the dynamical structure factor where the density of state is high. The density of state of rotons diverge at the roton minimum energy according to Eq. (4). This is the reason that the two-roton Raman peak at $2\Delta_0$ is the most dominant feature. Due to this fact, Raman scattering is suited specifically for study of roton excitations.

The Raman spectral feature in the energy shift region shown in Fig. 2(a) is well understood except for small details. With a suitable choice of the parameters, the Raman spectral shape can be calculated from the dynamical structure factor using Eqs. (2) and (3) with reasonable agreement with experiments,[4,13] although interactions between excitations slightly change detailed spectral features from those calculated from these equations.[13] The asymmetrical spectral shape of the two-roton Raman peak is evident from the dispersion relation of Eq. (4). There is no state below $2\Delta_0$, which results in an abrupt decrease of the spectrum. The two-roton states exist continuously above $2\Delta_0$, which contribute to the shoulder feature above $2\Delta_0$. Therefore, the asymmetricity does not mean that some excitations other than rotons are considerably contributing to the shoulder. The whole feature of the asymmetrical two-roton Raman scattering near $2\Delta_0$ comes from the single dispersion relation Eq. (4). However Eq. (4) is valid only for limited momentum region near q_0. For larger momentums, the dispersion relation approaches the plateau. And, as the momentum decreases from q_0, the dispersion relation approaches the local maximum; i.e., the maxon region. The Raman spectrum near 28 K would observe the contribution from two-maxon excitations. As mentioned in the Introduction, the two-maxon peak is absent due to small $t(\boldsymbol{q})$ (Ref. 4) and also

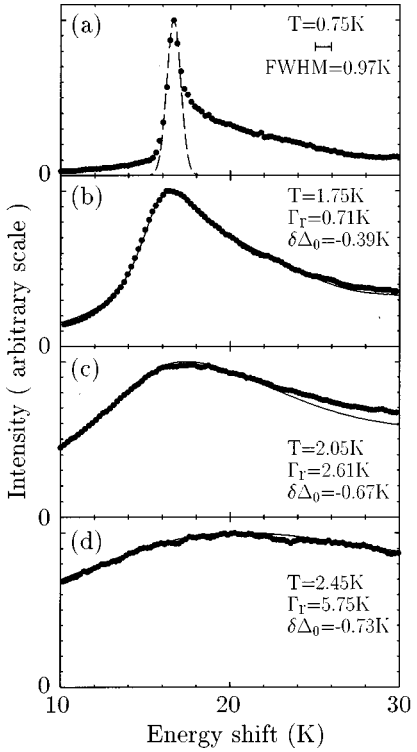

FIG. 4. Temperature dependence of the Raman spectrum of superfluid ^{4}He at the pressure of 4.9×10^5 Pa. The plot is similar to Fig. 2.

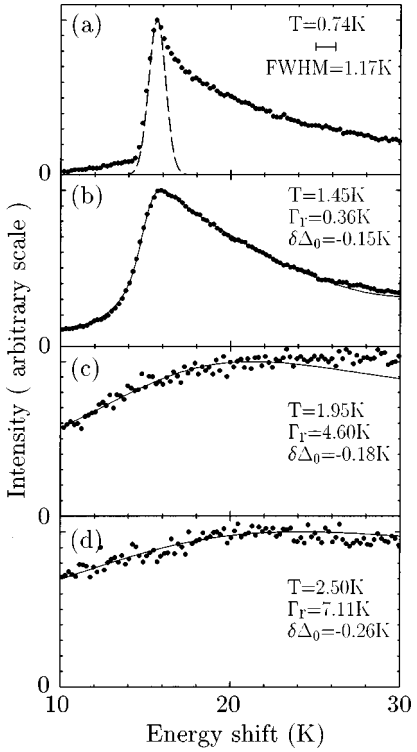

FIG. 5. Temperature dependence of the Raman spectrum of superfluid ^{4}He at the pressure of 1.96×10^6 Pa. The plot is similar to Fig. 2. The two-roton peak is highly asymmetric at this pressure.

possibly due to interactions between maxons.[13] The dominance of the two-roton Raman scattering validates analyses in this paper.

As mentioned in the Introduction, a few different models have been proposed to interpret temperature dependence of $S(q,\omega,T)$ measured by neutron inelastic scattering. Although we tried to analyze data using these models, we found that a simpler model can explain the present experimental results. In Fig. 1, broadening of the spectrum at 1.75 K is mainly due to temperature broadening. We found that the profile of the spectrum at the lower energy shift side of the two roton peak is fitted by a Lorentzian function. This fact suggests that the temperature broadening of the two-roton spectrum is Lorentzian broadening. The Lorentzian broadening is characteristic of the usual collision broadening of the spectrum. The probability of collision of a two-roton excited by incident laser with thermally excited rotons is proportional to an infinitesimal time interval at a constant rate. In such a case, the time decay of the two roton is exponential. The Fourier transform of an exponential time decay process results in a Lorentzian spectral form in the frequency domain. Therefore, the fact that the temperature broadening of the two-roton Raman scattering is described by Lorentzian broadening is consistent with the picture by Landau-Khalatnikov that the lifetime of rotons is determined by collisions with thermally excited rotons.[1]

Therefore we take into account the temperature effect on $S(q,\omega,0)$ near the roton region by a convolution integral with a Lorentzian function

$$L(\omega,\Gamma_r(T))=\frac{\Gamma_r(T)}{\pi}\frac{1}{\omega^2+\Gamma_r^2(T)}, \tag{5}$$

where $\Gamma_r(T)$ is the half width of a single roton. Then the dynamical structure factor $S(q,\omega,T)$ at a finite temperature T is related to $S(q,\omega,0)$ at absolute zero as

$$S(q,\omega,T)=\int_{-\infty}^{\infty}L(\omega-\omega'-\delta\Delta_0,\Gamma_r)S(q,\omega',0)d\omega', \tag{6}$$

where $\delta\Delta_0$ takes into account the variation of the roton minimum energy with temperature. If we substitute Eq. (6) for Eq. (3), the function $H(q,q',\omega,T)$ at a finite temperature T is related to $H(q,q',\omega,0)$ at absolute zero as

$$H(q,q',\omega,T)=\int_{-\infty}^{\infty}L(\omega-\omega'-2\delta\Delta_0,2\Gamma_r)\times H(q,q',\omega',0)d\omega'. \tag{7}$$

By substituting this relation into Eq. (2), we get

$$R(\omega,T)=\int_{-\infty}^{\infty}L(\omega-\omega'-2\delta\Delta_0,2\Gamma_r)R(\omega',0)d\omega', \tag{8}$$

for the temperature broadening of the Raman spectrum. Equation (6) and this relation show that the Raman spectrum broadens with a width twice that of the dynamical structure factor.

For the analysis over the wide energy shift region at various temperatures, the effect of the Bose factor must be taken into account.[17] The Bose factor for the Stokes component is $[1+n(\omega)]$, where the unity corresponds to excitations from the ground state and $n(\omega)$ is due to thermally excited excitations. The Bose factor of the anti-Stokes component is

$n(\omega)$. The Bose distribution gives $n(\omega)=[\exp(\omega/T)+1]^{-1}$. The higher the temperature is and the smaller the energy shift is, the larger the $n(\omega)$ is. Examples of numerical estimations are, at a temperature of 2 K, $n(\omega)\simeq 6.8\times 10^{-3}$ at an energy shift of $\omega=10$ K and $n(\omega)=4.5\times 10^{-5}$ at an energy shift of $\omega=20$ K. The factor $n(\omega)$ is practically negligible compared with unity in the present experimental region. In this experiment, all measurements were done on the Stokes component. Therefore, we set the Bose factor always equal to unity in all the analysis.

Other factors that might modify the relation of Eq. (8) are interactions between elementary excitations. If the created two rotons interact, theoretical Raman spectrum cannot be related to the dynamical structure factor in a simplified form like Eqs. (2) and (3).[19–21] The width of the two-roton bound state may not simply be equal to twice that of single roton. In fact, at very low temperatures, the two-roton bound state may decay directly into a phonon pair with same energy.[22] However, at the elevated temperatures concerned here, this decay is much slower compared with that due to collisions of a bound pair with thermally excited rotons. And also the early experiment, in which the temperature dependence of the two-roton bound state was measured, revealed that the width of Raman scattering is twice the width of single roton.[18] Then Eq. (8) is appropriate to estimate the single roton width $\Gamma_r(T)$ from Raman spectrum even for the interacting rotons.

In actual experiments, in addition to the temperature broadening, the instrumental resolution function also broadens spectra. Let the instrumental profile function be $P(\omega)$, which is shown by the dashed curve in Fig. 2(a). It was determined by the line shape of the central component. The shape is not exactly Gaussian, but is approximated by it well. Due to the instrumental broadening, the observed Raman spectrum $R_{\rm obs}(\omega,T)$ becomes

$$R_{\rm obs}(\omega,T)=\int_{-\infty}^{\infty}P(\omega-\omega')R(\omega',T)d\omega'. \qquad (9)$$

At a low enough temperature, the temperature width Γ_r is negligibly smaller than the instrumental width. Then the spectrum is broadened only by the latter. In Fig. 2(a), the spectrum observed at 0.8 K is broadened practically only by the instrumental width, because the dashed curve of the instrumental profile traces the experimental points near the peak maximum and at the lower energy shift side of the two roton peak. We can set $R_{\rm obs}(\omega,0)\simeq R(\omega,0.8\ {\rm K})$ for this case. Let the lowest temperature be written as $T_{\rm lst}$ for a series of measurements at a pressure. Then, from Eqs. (8) and (9), the observed spectrum at an arbitrary temperature T is

$$R_{\rm obs}(\omega,T)=\int_{0}^{\infty}L(\omega-\omega'-2\,\delta\Delta_0,2\Gamma_r)R_{\rm obs}(\omega',T_{\rm lst})d\omega'. \qquad (10)$$

This is the relation that we use for the analysis of our experimental data. We varied the width Γ_r and $\delta\Delta_0$ as adjustable parameters to find the best fit of this calculated spectral shape to the experimental spectrum at each temperature. The fit was judged near the peak and at the lower energy shift tail of the two-roton peak.

Three examples of fitting are shown in Figs. 2(b), 2(c), and 2(d) for three different temperatures at SVP. Figure 2(a) is the Raman spectrum measured at $T_{\rm lst}=0.8$ K, which is the lowest temperature of this measurement. In Fig. 2(b), the solid curve is obtained by the convolution integral of Eq. (10) with parameters $\Gamma_r=0.20$ K and $\delta\Delta_0=0$ K. The calculated curve can reproduce the experimental spectrum very well. In Fig. 2(c), the solid curve is the calculated result with $\Gamma_r=0.73$ K and $\delta\Delta_0=-0.20$ K. In this case also, the calculated curve can reproduce experimental spectrum well. For measurement at 2.15 K, shown in Fig. 2(d), a good fit was observed with parameters $\Gamma_r=2.58$ K and $\delta\Delta_0=-0.21$ K.

Fittings to determine Γ_r and $\delta\Delta_0$ are shown in Figs. 3, 4, and 5, respectively, for pressures of 9.8×10^4 Pa, 4.9×10^5 Pa, and 1.96×10^6 Pa. In these figures, (a) is the data at the lowest temperature $T_{\rm lst}$ and the broken curve is the instrumental profile. The parameters used for fitting are written in the figures.

We note a small deviation of the experimental data points from the calculated curve in (c) plot in the energy shift region larger than about 26 K in each figure. This region is no longer the two-roton region. Raman spectrum of superfluid ^{4}He is composed of contributions of multiphonon processes with zero total momentum. As such processes, in addition to the two-roton process, two-maxon, three-roton, and other processes are also conceivable. The two-maxon region is $\simeq 28$ K and the three-roton region is $\simeq 26$ K at SVP. Temperature broadening of these processes is different from that of the two-roton peak. Therefore, we determine the adjustable parameters by the best fit near the two-roton peak maximum and at its lower energy shift side, where contamination by other multiphonon processes is negligible.

The temperature dependences of the roton minimum energy $\Delta_0(T)$ are plotted in Figs. 6(a)–6(d), respectively, for pressures of SVP, 9.8×10^4 Pa, 4.9×10^5 Pa, and 1.96×10^6 Pa. The roton minimum energy decrease a little as the temperature approaches the λ transition temperature. Above the transition temperature, it is nearly constant.

At all pressures, as shown in Figs. 2–5, the maximum of the experimental spectrum is observed at larger energy shift as temperature increases. If we estimated the two-roton minimum energy simply at the peak maximum of the experimental spectrum, we came to regard that the two-roton energy increases as temperature increases. It is a misunderstanding. The two-roton Raman peak is antisymmetrical. The convolution integral of Eq. (10) measures the area of the spectrum which overlaps with the Lorentzian function. For an antisymmetrical peak, the area is larger for the side which has a stronger tail and the apparent peak maximum shifts toward this side as the Lorentzian width increases. This is the reason that the experimental peak maximum shifts to higher energy as temperature increases, although actual roton minimum energy decreases.

The temperature dependences of the roton half width $\Gamma_r(T)$ are plotted in Figs. 7(a)–7(d), respectively, for pressures of SVP, 9.8×10^4 Pa, 4.9×10^5 Pa, and 1.96×10^6 Pa.

The change of the peak height with temperature is also noted. The series of the spectra at 4.9×10^5 Pa depicted in Fig. 1 shows how the absolute peak intensity changes with temperature. The peak height decreases with an increase of temperature. We tested whether this change of the peak

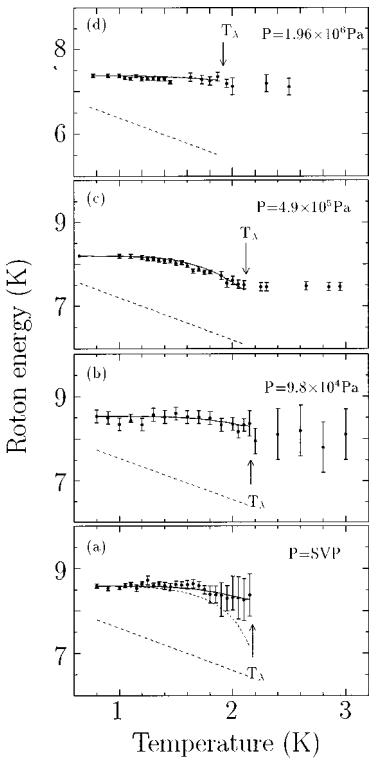

FIG. 6. Temperature dependence of the roton minimum energy of superfluid ^{4}He determined by Raman scattering at (a) SVP, (b) 9.8×10^4 Pa, (c) 4.9×10^5 Pa, and (d) 1.96×10^6 Pa. T_λ is the λ transition temperature. The solid curve is the best fit of Eq. (16) to determine the parameters *A*. The dashed line is the upper limit of $\Delta_0(T)$ imposed by the stability condition of Eq. (12). The broken line in the plot (a) is the theoretical prediction by BPF (Ref. 2).

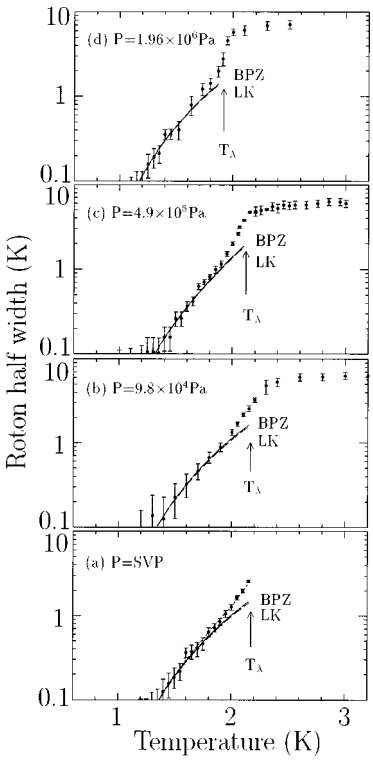

FIG. 7. Temperature dependence of the roton half width of superfluid helium ^{4}He determined by Raman scattering at (a) SVP, (b) 9.8×10^4 Pa, (c) 4.9×10^5 Pa, and (d) 1.96×10^6 Pa. The lower temperature values were fitted to the LK theory (the broken curve) and to Eq. (17) of the BPZ theory (the solid curve) to determine the parameter *B*. The dashed curve in the plot (a) is the theoretical prediction by BPZ in Ref. 3.

height can be explained by the simple Lorentzian broadening model. The Lorentzian function of Eq. (5) is normalized in the sense that integration of the function with ω gives unit. Let the half width of the spectrum at the lowest temperature, i.e., $T=0.75$ K in the case of Fig. 1, be $\Gamma_{\rm ins}$. At lower temperatures where $\Gamma_r(T)\ll\Gamma_{\rm ins}$, the convolution integral Eq. (10) does not change the spectrum shape as well as its peak intensity. As $\Gamma_r(T)$ becomes comparable with $\Gamma_{\rm ins}$, the convoluted spectrum starts broadening and the peak height decreases. At higher temperatures where $\Gamma_r(T)\gg\Gamma_{\rm ins}$, $\Gamma_r(T)$ determines the spectral broadening and the peak height is inversely proportional to it. This is due to the fact that the peak height of the Lorentzian, Eq. (5), at the maximum is inversely proportional to the $\Gamma_r(T)$.

We estimated $\Gamma_r(T)$ at an arbitrary temperature by drawing a smooth curve through experimental points in Figs. 7(a)–7(d). With these widths, the convolution integrals of Eq. (10) were carried out to estimate the temperature dependence of the peak height. The calculated peak height and the experimental peak height are compared in Figs. 8(a)–8(d), respectively, for pressures of SVP, 9.8×10^4 Pa, 4.9×10^5 Pa, and 1.96×10^6 Pa. In these plots, the vertical axis is normalized so that calculated peak height is unity at 1 K. The calculation can reproduce the experimental change of the peak height very well. The agreement of the calculated and observed peak heights are reasonable enough to validate the model analysis adopted here.

We compare the experimental results with theories. First of all, we discuss the conceptional theory by Griffin that the Bose condensate $n_0(T)$ introduces qualitative difference in $S(q,\omega,T)$ below the λ point. Various aspects of his theory are summarized in his review article[11] and also in his recent book.[12] Due to the existence of macroscopic condensate, density fluctuations have two different components; one is associated with the condensate and the other is not. The pair-correlation function of density fluctuations, $S(q,\omega,T)$ is also expected to have two terms. Because the term associated with the condensate exists only below the λ point, an additional term or some qualitative change in $S(q,\omega,T)$ is expected at the λ temperature. One of the experimental evidence was claimed by Wood and Svensson,[6] who introduced the two-fluid model of $S(q,\omega,T)$. They claimed that the superfluid component of $S(q,\omega,T)$ disappears just at the λ point as we approach it from below, analyzing their neutron data. However, as mentioned in the Introduction, a different interpretation was also proposed.[7] The question here is whether the temperature dependence of Raman spectrum indicates some effect of the Bose condensation or not.

From the facts that the strong sharp two-roton peak is only observed below the λ point as shown in Fig. 1, and also that the shape of the temperature dependence of the peak height shown in Fig. 8 is similar to the order parameter behavior in a second-order phase transition, one may be tempted to suppose that the strong two-roton peak might be associated with the dynamical structure factor of condensate origin. However, the fact that the Raman spectral shapes at

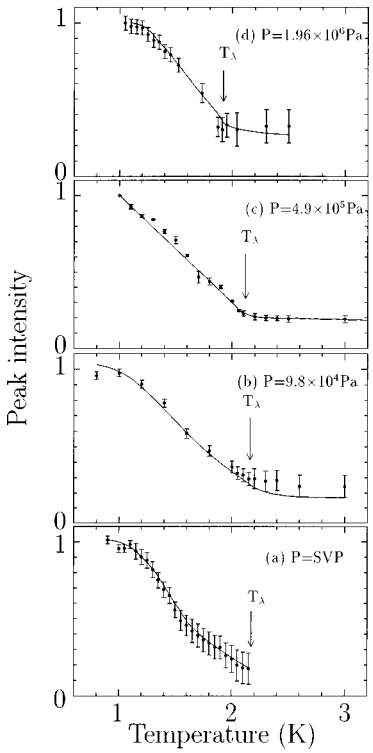

FIG. 8. Temperature dependence of the peak height of the two-roton Raman scattering at (a) SVP, (b) 9.8×10^4 Pa, (c) 4.9×10^5 Pa, and (d) 1.96×10^6 Pa. The vertical axis is suitably scaled so that the relative variation of the intensity is clearly displayed. The solid curve is the calculated value by the convolution integral of Eq. (10). For details see text.

elevated temperatures are all well described by Eq. (10), as shown in Figs. 2–5, means that there is no observable qualitative change in Raman spectral shape at the λ point. And the result that the temperature dependence of the Raman peak height is explained only by the broadening of the spectrum at all temperatures as depicted in Fig. 8, shows that there is no observable additional spectral component below the λ temperature. The sum rule, that the total Raman cross section is the same at all temperatures, is kept. The decrease of the peak height is only the result of spreading of the scattering process over wider energy shift regions. We could find no trace of the two-fluid model of $S(q,\omega,T)$ in our Raman data within our experimental accuracy.

The fact that we could detect neither any qualitative change in spectral shape nor any quantitative change in the total intensity at the λ point in our Raman-scattering experiment does not discard the possibility of Griffin's conceptional proposal that the Bose condensate affects $S(q,\omega,T)$. The condensate fraction is estimated to be less than 10%.[12] Small fractional change in $S(q,\omega,T)$ is more difficult to observe in Raman scattering because it is second order in $S(q,\omega,T)$ as shown in Eq. (3). There still remains the possibility of observing it with a more accurate Raman experiment.

Recent interpretation by Svensson, Montfrooij, and Schepper (SMS) on their neutron data is quite interesting in that they found disappearance of roton propagation just at the λ point.[23] A simple analogy with their interpretation is a harmonic oscillator with damping, familiar in textbooks of

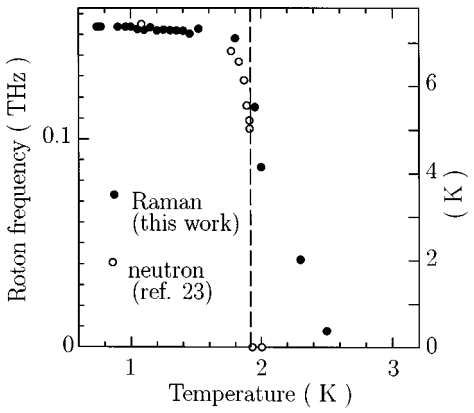

FIG. 9. Temperature dependence of the calculated roton frequency at the pressure of 1.96×10^6 Pa. The dots are from Raman scattering and the open circles are from neutron scattering. For details, see text.

classical dynamics. The oscillation frequency decreases with an increase of the damping and reaches the critical damping with zero oscillation frequency. Let us imagine that the harmonic frequency be the roton energy $\Delta_0(T)$ and the damping be the width $\Gamma_r(T)$. Although the roton minimum energy shows only weak temperature dependence as shown in Fig. 6, because the width increases markedly as shown in Fig. 7, the overdamping is expected at some temperature for roton propagations. SMS refers to the projection formalism to define the roton (propagation) frequency ω_r^p, which is $\mu_s(q,T)$ in their paper. The ω dependence of $S(q,\omega,T)$ is not a Lorentzian in the projection formalism, but can be approximated with it near the peak position. Then the width parameter z_u is approximately equal to $2\Gamma_r(T)$ in this paper. The roton frequency ω_r^p is then expressed as

$$\omega_r^p=[\Delta_0(T)^2-\Gamma_r^2]^{1/2}. \tag{11}$$

SMS made the experiment at a constant density which corresponds to the pressure of 1.96×10^6 Pa in this experiment. The roton frequency calculated with the equation for the Raman data is plotted with dots in Fig. 9 and compared with the neutron result by SMS with open circles. The roton frequency obtained from the neutron experiment becomes zero just at the λ point, which is the claim by SMS. On the contrary, the roton frequency calculated with the Raman-scattering data remains finite even above the λ point. It vanishes at about 2.6 K, about 0.7 K above the λ point. The difference comes from the difference in the value of the width $\Gamma_r(T)$ near the λ point. The Raman value is about one half of the neutron value. Concerning the discrepancy, discussion is given below.

Before discussion of the discrepancy, comparison with phenomenological theory by Bedell *et al.* is given. Temperature dependence of the roton minimum energy was estimated by Bedell, Pines, and Fomin (BPF) developing the roton liquid theory.[2] Later, Bedell, Pines, and Zawadowski (BPZ) extended the work with the pseudopotential theory.[3]

Using the roton liquid theory, BPF derived a stability condition for the normal fluid density, which provides the inequality for the roton minimum energy

$$\Delta_0(T)>\Delta_0(0)-T. \tag{12}$$

They pointed out that some experimental results derived from neutron experiments violate this inequality. The lower limit for $\Delta_0(T)$ is shown by dashed lines in Figs. 6(a)–6(d). The inequality is satisfied by all the present data derived from Raman-scattering experiments.

BPF's result for temperature dependence of the roton energy is

$$\Delta_0(T)=\Delta_0(0)+f_0N_r(T), \tag{13}$$

where $N_r(T)$ is the number of thermally excited rotons per unit volume. Their estimation from the specific heat at constant volume at SVP is $Nf_0=-9.67$ K, where N is the particle number density. The negative value of f_0 leads to a decrease of the roton minimum energy with an increase of temperature.

The experimental parameter $\Gamma_r(T)$ empirically introduced in Eq. (5) can be equalized to the theoretically calculated single-roton half width, which is the inverse of the roton lifetime. It is determined by scattering of rotons by other thermally excited rotons in the temperature region concerned here. Such an effect was theoretically calculated by Landau and Khalatnikov (LK) with Born approximation.[1] BPZ extended the work with the pseudopotential theory[3] and obtained

$$\Gamma_r(T)=\frac{q_0\mu_0\overline{w}}{4}N_r(T), \tag{14}$$

where $\overline{w}$ is the scattering rate.

The temperature dependences of both the roton minimum energy and the roton half width are determined by the number density of thermally excited rotons. Its temperature dependence was derived by BPF as[2]

$$N_r(T)=\frac{2q_0^2}{(2\pi)^{3/2}\hbar}\left[1+\alpha\frac{(\mu_0k_BT)^{1/2}}{\hbar}\right](\mu_0k_BT)^{1/2}\times\exp\left(-\frac{\Delta_0(T)}{k_BT}\right), \tag{15}$$

where the constant $\alpha=(2\pi)^{-1/2}(k_1^{-1}+k_2^{-1})$ takes into account the cubic correction [the third term on the right of Eq. (4)] to the roton dispersion curve. The original LK theory lacks this term. With this term, $\Gamma_r(T)$ of the BPZ theory takes values slightly larger than those of the LK theory as temperature increases.

The above temperature dependences are parametrically written as

$$\Delta_0(T)=\Delta_0(0)-A(1+CT^{1/2})T^{1/2}\exp(-\Delta_0(T)/T) \tag{16}$$

and

$$\Gamma_r(T)=B(1+CT^{1/2})T^{1/2}\exp(-\Delta_0(T)/T), \tag{17}$$

where the parameters A, B, and C are numerical constants and the energies are measured in K.

At SVP, BPZ estimated the parameters as $A=24.72$, $B=41.6$, and $C=0.0603$. Their theoretical estimations with these values are plotted in Figs. 6(a) and 7(a), respectively, for the roton minimum energy and the roton width. The roton widths show excellent agreement with the theoretical prediction of the dashed curve in Fig. 7(a). However, the experimental temperature dependence of the roton energy is about a half of their prediction as shown in Fig. 6(a) with the broken curve, although the experimental errors are large. In Eq. (16), the cubic correction $CT^{1/2}=0.085$ at 2 K being only a few percent, the magnitude of the temperature dependence is determined mainly by the factor A. A fit of our data to Eq. (16) with fixed $C=0.0603$ [the solid curve in Fig. 6(a)] yields $A=10\pm3$, which is about half the BPZ estimation. With these A and C values, fitting of Eq. (17) to our data at lower temperatures yields $B=43\pm3$, which agrees with BPZ estimation. However, the plot of Eq. (17) with these parameters deviates at a higher temperature region as shown by the solid curve in Fig. 7(a) due to weak temperature dependence of $\Delta_0(T)$.

TABLE I. Parameters to characterize the temperature dependence of the roton minimum energy and the roton half width in the expressions proposed by BPF and BPZ (Refs. 2 and 3). For details see Eqs. (15) and (16) in the text.

Pressure (Pa)	A	B	C
SVP	10 ± 3	43 ± 3	0.0603
9.8×10^4	7.5 ± 2	48 ± 3	0.0603
4.9×10^5	18 ± 2	40 ± 3	0.0588
1.96×10^6	3.8 ± 2	46 ± 3	0.0545

We estimated parameters A and B by the best fit of Eq. (16) and by a fit of Eq. (17) to data at low temperatures, respectively. The small cubic correction factor C was estimated following a BPF procedure from the neutron data of Dietrich *et al.*[24] The results are listed in Table I. The calculated roton minimum energy and width with these results are compared with experimental data with solid curves in Figs. 6 and 7. If we use temperature dependence of the roton minimum energy of the present experimental results to estimate the roton width in the framework of BPZ, the estimation yields weaker temperature dependence of the roton width at all pressures.

In Fig. 7, deviations of experimental data from BPZ theory to larger values are noticeable. The deviation suggests that a process which is not taken into account in their theory might play a role additionally to decrease the lifetime of rotons as we approach the λ point, while weak temperature dependence of the roton energy suggests such a process would not contribute to roton-roton interaction. Such a process may also work above the λ point because we note an increase of the width even above the λ point to certain values in Figs. 7(b)–7(d).

Another theoretical work also suggests existence excitations additional to rotons near the λ point. Reatto, Vitiello, and Masserini (RVM) introduced the shadow function theoretical method to calculate various quantities of superfluid ^{4}He at finite temperatures.[26] The method is very effective to take into account higher-order correlations in density fluctuations. For example, they obtained theoretical dynamical structure factors, which are in good agreement with experiments in its pressure and temperature dependence. However, the computed Bose condensate fraction is far from zero at the

experimental λ temperature. They pointed out that it suggests some excitations other than rotons become important near the λ point.

Griffin claimed that the roton peak intensity in $S(q,\omega,T)$ vanishes near the λ temperature, being replaced by a broad particle-hole spectrum which characterizes the normal phase.[12] And referring to our data,[16,25] he suggested that the deviation of $\Gamma_r(T)$ from the LK theory is related to it and that we cannot discuss the $\Gamma_r(T)$ near the λ transition in terms of the ''roton'' width. However, the fact in this experiment is that we can fit all the experimental spectra with Eq. (10) continuously up to above the λ temperature. And even concerning the neutron data, there are different interpretations as discussed in the Introduction. For example, in SMS's recent work referred to above, they interpret their neutron data that the roton propagation exists just up to the λ point. Apart from the conceptional discussion, only what we need to solve the discrepancy phenomenologically is that we can explain the deviation if there is some mechanism to increase the roton width additional to roton-roton scattering. And in fact there is a candidate as mentioned below.

Williams pointed out, as the superfluid density decreases near the λ point, energies of vortices decrease so that they are thermally excited. As the normal density decreases, vortex excitations come to dominate roton excitations to determine properties of liquid ^{4}He near the λ transition.[27]

One of the interesting aspects of this view is that vortices may exist in critical fluctuations of superfluid density. Although the average is zero, critical fluctuations in superfluid density exist even above the λ point. This may explain the continued increase of the roton width above the λ point as shown in Fig. 7.

RVM supported Williams's view of the vortex-induced λ transition. One reason is that it lowers the transition temperature from that calculated in their shadow function method. It may solve the question why the calculated Bose condensate fraction remains finite at the experimental λ point.

Another reason is that they could explain the discrepancy between Raman and neutron data by the vortex excitation model. The roton widths depicted in Fig. 7 agree with neutron results in those temperature regions where the BPZ theory traces the experimental points. However near the λ point, the widths observed by neutron scattering are large compared with those observed by Raman scattering. In the normal state apart from the λ point, the width observed by neutron scattering is about twice as large as the corresponding width observed by Raman scattering.

RVM explains as follows. In the presence of the superfluid velocity $\boldsymbol{v}_s$, the excitation energy $\varepsilon_r(\boldsymbol{q})$ is modified as $\varepsilon_r(\boldsymbol{q})' = \varepsilon_r(\boldsymbol{q}) + \hbar \boldsymbol{v}_s \cdot \boldsymbol{q}$. In the presence of a statistical distribution of vortices, the energy of a roton becomes distributed over larger and smaller values depending on the local value of $\boldsymbol{v}_s$ and on the direction of $\boldsymbol{q}$. This introduces an additional broadening mechanism which contributes to the dynamical structure factor measured by neutron scattering. For the case of Raman scattering, a pair of excitations are excited. Let the momentum of these excitations be $\boldsymbol{q}_1$ and $\boldsymbol{q}_2$, then the Raman shift $\omega = \varepsilon_r(\boldsymbol{q}_1)' + \varepsilon_r(\boldsymbol{q}_2)' = \varepsilon_r(\boldsymbol{q}_1) + \varepsilon_r(\boldsymbol{q}_2) + \hbar(\boldsymbol{q}_1 + \boldsymbol{q}_2) \cdot \boldsymbol{v}_s$. Because the momentum transfer of the Raman process is negligibly small compared with the roton momentum, $(\boldsymbol{q}_1 + \boldsymbol{q}_2) \simeq 0$. Therefore the effect of the existence of $\boldsymbol{v}_s$ is considerably small for Raman scattering compared with neutron scattering.

RVM calculated $S(q,\omega,T)$ using the theoretical model, which has the width Γ and the average superfluid velocity v_0 as adjustable parameters. They used Raman width $\Gamma = 1.9$ K from our Raman-scattering data[15] and chose $v_0 = 20$ m/s to calculate $S(q,\omega,T)$ at SVP, $T = 2.09$ K and $q = 1.925$ Å^{-1}. Their calculated result is in excellent agreement with neutron experiments.[7,8] This consistently explains apparent discrepancy between neutron and Raman results of the roton width.

The vortex excitation model by RVM seems promising to describe the dynamical behavior of ^{4}He near the λ point, although a more extensive comparison of calculated results with experiments are necessary to make a conclusive claim, as they point out. We believe, together with the BPZ theory for the relatively low-temperature region, a full phenomenological clarification of dynamic correlations in superfluid ^{4}He will become possible soon.

ACKNOWLEDGMENTS

We would like to thank to Professor M. Watabe and Professor K. Nagai for valuable discussion. Thanks are also due to T. Akagi and H. Yamashita for their partial collaboration on experiments. This work is supported by the cryogenic center of Hiroshima University and by a Grant-in-Aid for Scientific Research from the Ministry of Education, Science, and Culture of Japan.

*Present address: Chofu Laboratory, Kowa Company, Ltd., 3-3-1 Chofugaoka, Chofu-si, Tokyo 182-0021, Japan.

[1] I. M. Khalatnikov, *Introduction to the Theory of Superfluidity* (Benjamin, New York, 1965).

[2] K. Bedell, D. Pines, and I. Fomin, J. Low Temp. Phys. **48**, 417 (1982).

[3] K. Bedell, D. Pines, and A. Zawadowski, Phys. Rev. B **29**, 102 (1984).

[4] A. D. B. Woods and R. A. Cowley, Rep. Prog. Phys. **36**, 1135 (1973).

[5] E. C. Svensson, in *Elementary Excitations in Quantum Fluids*, edited by K. Ohbayashi and M. Watabe (Springer-Verlag, Berlin, 1989), p. 59.

[6] A. D. B. Woods and E. C. Svensson, Phys. Rev. Lett. **41**, 974 (1978).

[7] E. F. Talbot, H. R. Glyde, W. G. Stirling, and E. C. Svensson, Phys. Rev. B **38**, 11 229 (1988).

[8] W. G. Stirling and H. R. Glyde, Phys. Rev. B **41**, 4224 (1990).

[9] H. R. Glyde and A. Griffin, Phys. Rev. Lett. **65**, 1454 (1990).

[10] A. Griffin, Can. J. Phys. **65**, 1368 (1987).

[11] A. Griffin, in *Elementary Excitations in Quantum Fluids* (Ref. 5), p. 23.

[12] A. Griffin, *Excitations in a Bose-Condensed Liquid* (Cambridge University Press, Cambridge, 1993).

[13] T. Greytak, in *Quantum Liquids*, edited by J. Ruvalds and T. Regge (North-Holland, Amsterdam, 1978).

[14] K. Ohbayashi, in *Excitations in 2D and 3D Quantum Fluids*, edited by A. F. G. Wyatt and H. J. L. Lauter (Plenum, New York, 1991).

[15] H. G. M. Edwards, E. A. M. Good, and D. A. Long, J. Chem.

Soc., Faraday Trans. 2 **72**, 865 (1976).
[16] K. Ohbayashi, M. Udagawa, H. Yamashita, M. Watabe, and N. Ogita, Physica B **165&166**, 485 (1990).
[17] W. Hayes and R. Loudon, *Scattering of Light by Crystals* (Wiley, New York, 1978).
[18] T. Greytak and J. Yan, Phys. Rev. Lett. **22**, 987 (1969).
[19] J. Ruvalds and A. Zawadowski, Phys. Rev. Lett. **25**, 333 (1970).
[20] F. Iwamoto, Prog. Theor. Phys. **44**, 1135 (1970).
[21] T. Greytak, R. Woerner, J. Yan, and R. Benjamin, Phys. Rev. Lett. **25**, 1547 (1970).
[22] J. Yau and M. J. Stephen, Phys. Rev. Lett. **27**, 482 (1971).
[23] E. C. Svensson, W. Montfrooij, and I. M. de Schepper, Phys. Rev. Lett. **77**, 4398 (1996).
[24] O. W. Dietrich, E. H. Graf, C. H. Huang, and L. Passell, Phys. Rev. A **5**, 1377 (1972).
[25] K. Ohbayashi, in *Elementary Excitations in Quantum Fluids* (Ref. 5), p. 32.
[26] L. Reatto, S. A. Vitiello, and G. L. Masserini, J. Low Temp. Phys. **93**, 897 (1993).
[27] G. A. Williams, Phys. Rev. Lett. **59**, 1926 (1987); **68**, 2054 (1992).